First publ. in: Journal of Geophysical Research 107 (2002), , No. C12, 3230

Application of k-ϵ turbulence models to enclosed basins: The role of internal seiches

G.-H. Goudsmit
Swiss Federal Institute for Environmental Science and Technology (EAWAG), Dübendorf, Switzerland

H. Burchard
Institute for Oceanography, University of Hamburg, Hamburg, Germany

F. Peeters and A. Wüest
Swiss Federal Institute for Environmental Science and Technology (EAWAG), Dübendorf, Switzerland

Received 4 May 2001; revised 14 March 2002; accepted 4 April 2002; published 26 December 2002.

[1] A numerical model was developed for the prediction of the density stratification of lakes and reservoirs. It combines a buoyancy-extended k-ϵ model with a seiche excitation and damping model to predict the diffusivity below the surface mixed layer. The model was applied to predict the seasonal development of temperature stratification and turbulent diffusivity in two medium-sized lakes over time periods ranging from 3 weeks to 2 years. Depending on the type of boundary condition for temperature, two or three model parameters were optimized to calibrate the model. The agreement between the simulated and the observed temperature distributions is excellent, in particular, if lake surface temperatures were prescribed as surface boundary condition instead of temperature gradients derived from heat fluxes. Comparison of different model variants revealed that inclusion of horizontal pressure gradients and/or stability functions is not required to provide good agreement between model results and data. With the aid of uncertainty analysis it is shown that the depth of the mixed surface layer during the stratified period could be predicted accurately within ±1 m. The sensitivity of the model to several parameters is discussed. *INDEX TERMS:* 4211 Oceanography: General: Benthic boundary layers; 4255 Oceanography: General: Numerical modeling; 4568 Oceanography: Physical: Turbulence, diffusion, and mixing processes; *KEYWORDS:* lake, turbulence model, seiche, stratification, simulation, turbulence kinetic energy

Citation: Goudsmit, G.-H., H. Burchard, F. Peeters, and A. Wüest, Application of k-ϵ turbulence models to enclosed basins: The role of internal seiches, *J. Geophys. Res.*, *107*(C12), 3230, doi:10.1029/2001JC000954, 2002.

1. Introduction

[2] One of the major goals of environmental science is to determine the spatial and temporal development of chemical constituents originating from natural or anthropogenic sources in an ecosystem. To understand and to predict the fate of such substances in lakes, physical transport is one of the dominating factors. For this purpose, many numerical lake models have been constructed in the past. Most of them are one-dimensional and are able to describe vertical variations of physical and chemical parameters. The assumption of the one dimensionality is justified for lakes of small or medium size as horizontal variations of temperature and concentrations of substances are not significant in most cases, because vertical transport in density stratified lakes is about 10^3–10^5 times smaller than the horizontal one [e.g., *Imboden and Wüest*, 1995]. Furthermore, transformation processes of water constituents originating from a point source simulated by a one-dimensional approach must be slower then horizontal transport as otherwise horizontal gradients may occur.

[3] The structure of the hydrodynamical part of one-dimensional lake models can be classified in the following two categories.

1. Advective-diffusive models with simple parameterization schemes or given rates for vertical transport. Typical representatives are SEEMOD [*Zamboni et al.*, 1992], Minlake [*Riley and Stefan*, 1987], CHEMSEE [*Ulrich*, 1991], LIMNMOD [*Karagounis et al.*, 1993], and PROTECH [*Reynolds and Irish*, 1997; *Elliot et al.*, 1999]. These models are relatively simple to develop and require often less input data and are well suited for biochemical and geochemical studies in which chemical and biological processes have no considerable effect on transport. On the other hand, such models are rather empirical and model-specific parameters are introduced which are difficult to justify and to determine.

2. Models based on turbulence closure schemes, where rates for vertical transport are not directly parameterized by

Konstanzer Online-Publikations-System (KOPS)
URL: http://www.ub.uni-konstanz.de/kops/volltexte/2007/4386/
URN: http://nbn-resolving.de/urn:nbn:de:bsz:352-opus-43868

external forces but are related to the turbulent kinetic energy. Typical representatives of this category are for instance the bulk model of *Kraus and Turner* [1967], DYRESM [*Imberger and Patterson*, 1981], PROBE [*Svensson*, 1978; *Huttula et al.*, 1992; *Svensson*, 1998; *Elo et al.*, 1998], GOTM [*Burchard et al.*, 1999], and other k-ϵ models [e.g., *Burchard and Baumert*, 1995]. These models are derived from hydrodynamical equations and are able to simulate transport processes quite accurately with high temporal resolution but are more difficult to develop and calculations are more time consuming. However, models of this type allow predictions of the effect of climatic change on vertical mixing and also the interaction of chemical, biological, and physical processes can be studied. Moreover, such models have usually a higher temporal resolution as models of type A and are also well suited for investigations of transport and fast transformation processes within the mixed layer. Since the rapid improvement of computer capacity in the last years, models of type B can easily be applied in even long-term studies.

[4] The model presented here belongs to the category 2. Most of the models based on turbulence closure schemes focus on an adequate prediction of the mixed layer depth, a task that is usually satisfactorily performed as long as the forcing is well known. However, in the stratified water below, such models often predict negligible turbulent kinetic energy resulting in molecular values for viscosity and diffusivities. But in fact, experimental observations in many deep lakes revealed a very high level of diffusivity on the order of $cm^2\ s^{-1}$ [*Wüest and Gloor*, 1998] and up to tens of $cm^2\ s^{-1}$ [*Ravens et al.*, 2000; *Crawford and Collier*, 1997]. Such values lead to transport of water constituents, such as oxygen, that is 10^5 to 10^6 times molecular transport. The sources of the turbulence for such mixing has been identified by experimental observations [*Imberger*, 1998]: It is pelagic shear-induced turbulence, responsible for mixing in the interior of the upper pycnocline and turbulence generated at the bottom as a result of the interaction with the hypolimnetic currents. The first contribution is explained by the fact that part of the kinetic energy introduced into the water surface by wind is transferred to internal motions (such as internal basin-scale seiches as well as high-frequency internal waves) and becomes therefore indirectly available for turbulent mixing in the interior.

[5] The present approach was motivated by turbulence measurements and dye tracer experiments in Lake Alpnach, which showed that (1) hypolimnetic dissipation rates increased according to wind excitation and decayed with a typical time constant of a few days [*Gloor et al.*, 2000] and (2) that vertical mixing in the hypolimnion was found to be predominantly determined by mixing near the bottom boundary [*Wüest et al.*, 1996; *Goudsmit et al.*, 1997], a fact that has been confirmed by many others [*Lemckert and Imberger*, 1998; *MacIntyre et al.*, 1999; *Ravens et al.*, 2000; *Antenucci et al.*, 2000].

[6] Therefore the lake model presented comprises not only a k-ϵ turbulence closure scheme but also an additional seiche excitation and damping model. This seiche model with wind forcing and bottom friction as energy source and sink, respectively, is added to estimate the diffusivity below the surface boundary layer of the enclosed basin.

[7] In a first application, the seasonal development of temperature stratification and turbulent diffusivity in Lake Baldegg was simulated employing different variants of the k-ϵ model. In addition, a sensitivity analysis is employed to estimate the absolute and relative contribution of model parameters and boundary conditions to the model results. In a second application, the temperature development in Lake Alpnach was simulated. It is shown that the lake model is able to predict adequately not only the temperature variations but also the absolute values and the vertical structure of the turbulent diffusivity. From these two applications it can be concluded that the lake model is well appropriate for the simulation of vertical transport and density stratification in deep stratified basins.

2. Model Approach

2.1. Basic Model

[8] The model is based on the buoyancy-extended k-ϵ model [*Rodi*, 1984] to describe the vertical density structure and mixing. As this has been already described in detail elsewhere [e.g., *Burchard et al.*, 1998], we confine ourselves to a brief description of the framework.

[9] The one-dimensional model equations are based on the assumption that horizontal gradients are negligible, which is usually fulfilled for small or medium-sized basins. In lakes and reservoirs, the horizontal structure of currents is not uniform and is, consequently, beyond the scope of this one-dimensional model. River intrusions are not included in this model version and, consequently, terms for vertical advection were omitted. In the one-dimensional vertical model (z axis positive upwards) the basic set of equations for temperature T [°C], mean horizontal velocity components u and v [m s^{-1}] with respect to x and y [m], turbulent kinetic energy (TKE) per unit mass k [J kg^{-1}], and the TKE dissipation rate ϵ [W kg^{-1}], are

$$\frac{\partial T}{\partial t} = \frac{1}{A}\frac{\partial}{\partial z}\left(A\left(\nu_t' + \nu'\right)\frac{\partial T}{\partial z}\right) + \frac{1}{\rho_0 c_p}\frac{\partial H_{sol}}{\partial z} + \frac{dA}{dz}\frac{H_{geo}}{A\rho_0 c_p} \tag{1}$$

$$\begin{aligned} \frac{\partial u}{\partial t} &= \frac{1}{A}\frac{\partial}{\partial z}\left(A(\nu_t + \nu)\frac{\partial u}{\partial z}\right) + fv \\ \frac{\partial v}{\partial t} &= \frac{1}{A}\frac{\partial}{\partial z}\left(A(\nu_t + \nu)\frac{\partial v}{\partial z}\right) - fu \end{aligned} \tag{2}$$

$$\frac{\partial k}{\partial t} = \frac{1}{A}\frac{\partial}{\partial z}\left(A\nu_k\frac{\partial k}{\partial z}\right) + P + P_{Seiche} + B - \epsilon \tag{3}$$

$$\frac{\partial \epsilon}{\partial t} = \frac{1}{A}\frac{\partial}{\partial z}\left(A\nu_\epsilon\frac{\partial \epsilon}{\partial z}\right) + \frac{\epsilon}{k}\left(c_{\epsilon 1}(P + P_{Seiche}) + c_{\epsilon 3}B - c_{\epsilon 2}\epsilon\right) \tag{4}$$

where ρ_0 [kg m^{-3}] and c_p [J kg^{-1} K^{-1}] represent a reference density and specific heat of lake water, respectively. A is the surface area of the lake at depth z, H_{sol} [W m^{-2}] the shortwave solar radiation penetrating the water, H_{geo} [W m^{-2}] the geothermal heat flux, and f [s^{-1}] the Coriolis parameter. ν and ν_t are molecular and turbulent viscosity (momentum), ν_t' and ν' are molecular and turbulent diffusivity of temperature, and ν_ϵ and ν_k

Table 1. Parameters of the k-ϵ Lake Model

Model Constant	Value	Calibrated Model Parameter	Value
$c_{\epsilon 1}$	1.44	p_1 (Lake Baldegg)	1.18
$c_{\epsilon 2}$	1.92	p_2 (not optimized)	1.0
$c_{\epsilon 3}$ ($B < 0$)	−0.4		
$c_{\epsilon 3}$ ($B > 0$)	1.0	α (Lake Alpnach)	1.7×10^{-3}
σ_ϵ	1.3	α (Lake Baldegg, H_{net})	6.2×10^{-3}
σ_k	1.00	α (Lake Baldegg, *SST*)	6.3×10^{-3}
c_μ	0.09		
c'_μ	0.072	q (Lake Alpnach)	0.77
ν'	1.5×10^{-7} m^2 s^{-1}	q (Lake Baldegg, H_{net})	0.88
ν	1.5×10^{-6} m^2 s^{-1}	q (Lake Baldegg, *SST*)	1.02
H_{geo}	0.1 W m^{-2}		
C_{Deff}	2×10^{-3}		
z_0 (*surface*)	0.5		
z_0 (*bottom*)	0.05		
ϵ_{water}	0.3 m^{-1}		
β	0.00033 m^2 mg POC^{-1}		
r_s	0.2		
κ	0.41		

[m^2 s^{-1}] are the turbulent diffusivities of energy dissipation and TKE, respectively. The shear stress production P [W kg^{-1}] and the buoyancy production B [W kg^{-1}] are given by

$$P = \nu_t \left(\left(\frac{\partial u}{\partial z}\right)^2 + \left(\frac{\partial v}{\partial z}\right)^2 \right) \qquad B = -\nu'_t N^2 \tag{5}$$

where N is the Brunt-Väisälä frequency defined by

$$N^2 = -\frac{g}{\rho_0}\frac{\partial \rho}{\partial z}. \tag{6}$$

P_{Seiche} [W kg^{-1}], discussed in the next section, is the production of TKE due to internal seiching. The turbulent viscosity and diffusivity can be calculated using the relation of Kolmogorov and Prandtl

$$\nu_t = c_\mu \frac{k^2}{\epsilon} \qquad \nu'_t = c'_\mu \frac{k^2}{\epsilon} \tag{7}$$

The turbulent diffusivities for k and ϵ are

$$\nu_k = \frac{c_\mu}{\sigma_k}\frac{k^2}{\epsilon} \qquad \nu_\epsilon = \frac{c_\mu}{\sigma_\epsilon}\frac{k^2}{\epsilon} \tag{8}$$

with $c_{\epsilon 1}$, $c_{\epsilon 2}$, $c_{\epsilon 3}$, c_μ, c'_μ, σ_k, and σ_ϵ being model constants listed in Table 1.

[10] In equation (2) horizontal pressure gradients were not included. We discuss this assumption later in the paper. In equation (5) the buoyancy term B can be a sink of TKE for stable stratification or a source of TKE for unstable water columns. The latter is the case for convection where an increase in TKE intensifies diffusivity.

2.2. Turbulence Induced by Internal Seiches

2.2.1. Model for the Energy Balance of Internal Seiches

[11] In the water below the epilimnion the production of TKE directly by wind stress is of minor importance during periods of strong stratification, for example, during the summer month in temperate lakes. During such periods kinetic energy input from wind forcing is transferred to the deep water mainly via internal seiche motions. The damping of the seiche motion, i.e., the loss of seiche energy by friction, is the main source of TKE below the epilimnion. To incorporate the seiche-induced production of TKE in our k-ϵ model, we included, based on ideas of *Gloor et al.* [2000], a simple description of the energy balance for the internal seiche motion:

$$\frac{dE_{seiche}}{dt} = PW - LS \tag{9}$$

where E_{seiche} [J] is the total energy of the seiche motion, PW [W] the production of seiche energy by wind forcing and LS [W] the loss of internal seiche energy by friction.

[12] The production and the loss of seiche energy are modeled by empirical relations which are motivated by experimental observations in lakes. Because the seiche motion is excited by wind forcing the energy transferred to the seiche is assumed to be proportional to the total energy introduced at the lake surface by wind forcing:

$$PW = \alpha A_0 \rho_{air} c_{10} \left(u_{10}^2 + v_{10}^2\right)^{3/2} \tag{10}$$

where A_0 [m^2] is the surface area of the lake, ρ_{air} [kg m^{-3}] the density of air, u_{10} and v_{10} [m s^{-1}] the East and North component of wind speed measured at 10 m height above the water surface, and c_{10} [-] the drag coefficient. The constant of proportionality α [-] is a model parameter which gives the fraction of the total wind energy introduced at the lake surface which is transferred to the seiche motion. In general the model parameter α is subject to model calibration.

[13] Friction within the water body and at the lake boundaries results in a loss of energy from the seiches, LS, which can be observed especially after strong excitation as a damping of the seiche oscillations and a decay of the associated velocity amplitudes. Experimental studies have shown that in the deep water the energy dissipation is approximately two orders of magnitude larger at the bottom boundaries than in the open water [*Wüest et al.*, 1996]. In addition, *Goudsmit et al.* [1997] have demonstrated that vertical mixing of a passive tracer in the open water is small compared to vertical mixing at the bottom boundaries. Because in the hypolimnion the energy source to drive vertical mixing is the seiche energy, it is reasonable to assume that the loss of energy occurs mainly at the basin boundaries as a result of bottom friction [*Gloor*, 1995]. Assuming a logarithmic velocity profile above the bottom boundaries the loss of energy is proportional to the velocity to the power of 3, or to kinetic energy to the power of 3/2. Based on these considerations the loss of seiche energy is modeled as

$$LS = -\gamma E_{seiche}^{3/2} \tag{11}$$

where γ [m^{-1} kg$^{-1/2}$] is a constant of proportionality which depends on the bottom friction and the basin geometry.

[14] The parameter γ can be estimated as follows: The temporal mean of the total energy contained in the seiche

motion can be determined from water velocities associated with the seiching

$$\overline{E_{seiche}} = 2\int_{z_{bottom}}^{z_{surf}} A\rho\overline{\frac{1}{2}u_{seiche}^2}dz \approx V_0\rho_0\overline{u_{seiche}^2} \tag{12}$$

and V_0 is the volume of the basin and u_{seiche} represents the velocity due to the seiche motion which is assumed to be independent of depth. The overbar indicates the long term average which extends over one or several seiche periods. Typically, $|\overline{u_{seiche}}|$ is on the order of a few cm s^{-1}. Thus, in Lake Alpnach ($V_0 = 1.0 \times 10^8$ m^3, $A_0 = 4.76 \times 10^6$ m^2, $|\overline{u_{seiche}^2}| \approx (0.03$ m s$^{-1})^2$) the total seiche energy is about 1×10^8 J.

[15] Assuming that the energy loss LS is entirely caused by bottom friction

$$\gamma\overline{E_{seiche}^{3/2}} \approx A_{boundary}\rho_0 C_{Deff}\overline{|u_{seiche}|^3} \tag{13}$$

where $A_{boundary}$ is the area of the bottom boundary of the lake and C_{Deff} [-] is the effective bottom friction coefficient assumed to be independent of depth. In good approximation the area of the bottom boundary $A_{boundary}$ can be approximated by the surface area A_0 assuming that the slope of the boundary is small. From equations (12) and (13) follows

$$\gamma \approx A_0 V_0^{-3/2}\rho_0^{-1/2}C_{D_{eff}}. \tag{14}$$

Assuming that C_{Deff} corresponds to the local bottom friction coefficient at 1 m height above the bottom $C_D \approx 0.002$ [*Elliot*, 1984] one obtains for Lake Alpnach $\gamma \approx 2 \times 10^{-10}$ m^{-1} kg$^{-1/2}$.

[16] Using equations (14), (10), and (11), the seiche energy balance, equation (9) can be rewritten

$$\frac{dE_{seiche}}{dt} = \alpha A_0\rho_{air}c_{10}\left(u_{10}^2 + v_{10}^2\right)^{3/2} - C_{D_{eff}}A_0V^{-3/2}\rho_0^{-1/2}E_{seiche}^{3/2} \tag{15}$$

The estimation of γ based on the bottom friction with $C_{D_{eff}} \approx 0.002$ can be checked for consistency by deriving the half-life $\tau_{E_{seiche}}$ of the seiche energy from γ and comparing it to observations. If the seiche motion has been excited and the wind forcing stops, the energy contained in the seiche motion should decay according to our model as

$$\frac{dE_{seiche}}{dt} = -\gamma E_{seiche}^{3/2} \tag{16}$$

The solution of equation (16) is given by

$$E(t) = \left(\frac{1}{\sqrt{E(t=0)}} + \frac{\gamma}{2}t\right)^{-2} \tag{17}$$

from which follows

$$\tau_{E_{seiche}} = \frac{2\left(\sqrt{2}-1\right)}{\gamma\sqrt{E(t=0)}} \tag{18}$$

Note, that according to equation (18) the seiche motion decays faster the more energy it contains. According to the estimations above, in Lake Alpnach $E_{seiche} \approx 1 \times 10^8$ J and $\gamma \approx 2 \times 10^{-10}$ m^{-1} kg$^{-1/2}$. Thus, the half-life of seiche energy $\tau_{E_{seiche}} \approx 3$ days, which is in reasonable agreement with observations by *Gloor et al.* [2000]. Thus, a $C_{D_{eff}} \approx 0.002$ provides consistent results for the loss of seiche energy by bottom friction and the half-life of seiche energy.

[17] The order of magnitude of α can also be estimated from the energy balance of the seiche motion. Because over long time periods the total seiche energy remains approximately constant production and loss of seiche energy must be approximately the same in the long term average. Thus, α can be estimated from equations (13) and (10):

$$\alpha \approx \frac{\rho_0 C_{D_{eff}}\overline{|u_{seiche}|^3}}{\rho_{air}c_{10}W_{10}^3} \tag{19}$$

and $W_{10} = \overline{\left(\left(u_{10}^2 + v_{10}^2\right)^{3/2}\right)^{1/3}}$ [m s^{-1}]. Because c_{10} is on the order 1×10^{-3} it follows that $\alpha \approx 2000\left(\frac{|\overline{u_{seiche}}|}{W_{10}}\right)^3$. With typical values in Lake Alpnach of 3 ms^{-1} for W_{10} and a value of 0.03 ms^{-1} for $|\overline{u_{seiche}}|$ one obtains $\alpha \approx 2 \times 10^{-3}$, well among experimental values [*Wüest et al.*, 2000].

2.2.2. Production of Turbulent Kinetic Energy by the Seiche Motion

[18] To describe the production of turbulent kinetic energy due to damping of the seiche motion as a function of depth we make the following assumptions: (1) the kinetic energy of the seiche motion is transformed into turbulent kinetic energy and heat; (2) because the loss of seiche energy occurs predominantly at the boundaries due to bottom friction, the generation of turbulent kinetic energy is proportional to the bottom area at a given depth; and (3) the production of TKE per unit time and unit area of the bottom boundary $P_{Seiche,sed}$ [W m^{-2}] is independent of depth. A considerable part of the kinetic energy of the seiche motion is dissipated within the viscous sublayer on a molecular level ($\approx 10\sqrt{C_{D_{eff}}} \approx 40\%$ [*Imboden and Wüest*, 1995] and is not available for the production of TKE. Under these assumptions

$$P_{Seiche,sed} = \frac{1}{A_{boundary}}\gamma E_{seiche}^{3/2}\left(1 - 10\sqrt{C_{D_{eff}}}\right) \tag{20}$$

where $A_{boundary}$ represents the total bottom area. The production of TKE per unit time and mass P_{Seiche} [W kg^{-1}] is therefore given by

$$P_{Seiche}(z) \sim \frac{1}{A}\frac{dA}{dz}\frac{1}{\rho_0}P_{Seiche,sed} \tag{21}$$

As TKE in the hypolimnion of lakes is mainly generated near the bottom boundaries, the question arises how it is transported from the boundary region into the open water, where the water column is stratified, and how turbulence can result in mixing. Based on observations in Lake Alpnach [*Gloor et al.*, 2000] developed a model according to which periodic intrusions from the bottom boundaries into the lake interior are the major cause for the basin-wide diapycnal mixing observed. Their analysis is based on the theory of *Barenblatt* [1978] describing intrusions in a stably stratified fluid. The intrusions are driven by horizontal pressure gradients induced by the difference between the density of

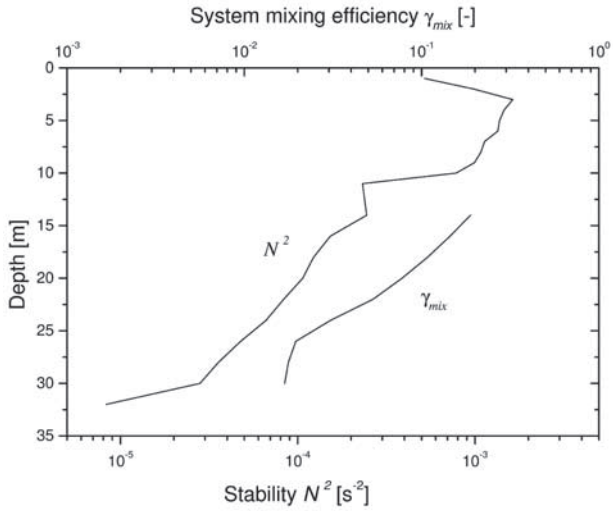

Figure 1. System mixing efficiency γ_{mix} and stability N^2 as a function of depth in Lake Alpnach. The values are averaged for the period May 26 until July 21, 1994. Adapted from *Gloor et al.* [2000].

the water in the mixed boundary layer and that in the stratified interior. According to *Gloor et al.* [2000] the horizontal intrusion velocity is proportional to N^2. *Gloor et al.* [2000] were also able to show that for typical scenarios the intrusions are able to penetrate the interior water column and thus to affect the vertical transport process of the entire basin.

[19] The buoyancy flux in a certain depth range, associated with the density intrusions from the bottom boundary, depends on the local generation mechanisms of the intruding water masses. In case of a well-mixed bottom boundary layer, the action of boundary turbulence is to remix already mixed water, which is an inefficient process in respect of buoyancy flux production, as explained by *Garrett* [1990]. If the stratification reaches all the way to the bottom interface, the buoyancy production reaches its maximum [*Wüest and Gloor*, 1998] since turbulence in a logarithmic layer is highest closest to the bottom. Mixing efficiency, expressed as the fraction of turbulent kinetic energy which produces buoyancy, can be expected to depend on stratification N^2. Indeed, based on current and turbulence measurements, *Gloor et al.* [2000] found that the basin-wide mixing efficiency (averaged over the entire basin within a certain depth range), the so-called system mixing efficiency (Figure 1), decreases with the stratification N^2.

[20] Motivated by these theoretical considerations and empirical findings, we parameterize the flux of seiche-induced TKE, which is available for buoyancy production (i.e., available for mixing), with the stability of the water column N^2. Combining this with equation (21) the horizontal mean of the TKE produced per unit time and mass which originates from the loss of seiche energy and which is available for mixing by the empirical relation:

$$P_{Seiche}(z) = cN^{2q}\frac{1}{A}\frac{dA}{dz}\frac{1}{\rho_0}P_{Seiche,sed} \tag{22}$$

where q [-] is a positive empirical parameter which has to be adjusted for each lake and c [s^{2q}] is a normalization constant. The term N^{2q} accounts for the intrusion of mixed water from the bottom boundaries into the open water. We assume that the part of seiche energy which is not dissipated in the molecular sublayer is transferred to TKE, i.e.,

$$\int_{z_{bottom}}^{z_{surf}} A\rho_0 P_{seiche}(z)\,dz = \gamma E_{seiche}^{3/2}\left(1 - 10\sqrt{C_{D_{eff}}}\right) \tag{23}$$

By combining equations (22), (23), and (20) the production of TKE by the seiche motion can be described as

$$P_{Seiche}(z) = \frac{1 - 10\sqrt{C_{D_{eff}}}}{\rho_0 c A_{boundary}} N^{2q}\frac{1}{A}\frac{dA}{dz}\gamma E_{seiche}^{3/2} \tag{24}$$

2.3. Boundary Conditions

2.3.1. Temperature

[21] At the surface the net heat flux H_{net} can be used as boundary condition (Neumann type) for the temperature equation

$$\rho_0 c_p\left(\left(\nu_t' + \nu'\right)\frac{\partial T}{\partial z}\right)_{z_{surf}} = H_{net}. \tag{25}$$

It should be noted that H_{net} does not contain the shortwave radiation from the sky H_{sol}. H_{sol} is included in equation (1) as a separate production term. The net heat exchange H_{net} between atmosphere and water consists mainly of four components

$$H_{net} = H_A + H_W + H_V + H_C \tag{26}$$

where H_A is the infrared radiation from the sky, H_W the infrared radiation emitted from the water, H_V the flux of latent heat and H_C the flux of sensible heat. These heat fluxes are defined to be positive if heat flows from the atmosphere into the water. Heat fluxes induced by precipitation and the effects of the throughflow of water by inlets and outlets are generally small and are therefore neglected [*Livingstone and Imboden*, 1989]. The different fluxes were calculated from atmospheric temperature, lake surface temperature, wind speed, atmospheric water vapor pressure, water vapor saturation pressure at the lake surface temperature and cloud cover using the bulk formulae of *Livingstone and Imboden* [1989] (Table 2).

[22] One of the crucial requirements for the model using this type of boundary condition for temperature are correct heat fluxes which are often difficult to determine. Inaccurate heat fluxes could easily lead to incorrect interpretation of the results if a number of other parameters is simultaneously estimated. The main difficulty for the determination of H_{net} is the fact that H_{net} is a superposition of various components, where each of them has to be calculated by its own set of coefficients. Moreover, H_{net} is mainly determined by the difference of infrared radiation from the sky and from the water surface. Because the absolute values of these two terms are much larger than H_{net} and due to the cumulative uncertainties of the parameters involved, the uncertainty of H_{net} can be quite significant ($\approx$20 W m^{-2}). The

Table 2. Thermal Energy Fluxes at Water Surface

Model Constant	Value	Unit	Remarks
	Infrared Radiation From Sky		
H_A	$p_1\ (1 - r_A)E_A\sigma T_A^4$	Wm^{-2}	
r_A	0.03	-	reflection of infrared radiation from water
E_A	$1.24\ (1 + 0.17C^2)\ \left(\frac{e_a}{T_A}\right)^{1/7}$	-	emissivity of atmosphere
C		-	cloud coverage
σ	5.67×10^{-8}	$W\ m^{-2}\ K^{-4}$	Stefan-Boltzmann constant
T_A		K	absolute atmospheric temperature
e_a		mbar	atmospheric water-vapor pressure
p_1	≈ 1.0	-	fit parameter
	Infrared Radiation From the Water Surface		
H_W	$-E_W\sigma T_W^4$	Wm^{-2}	
E_W	0.97	-	emissivity of water
T_W		K	absolute temperature of water surface
	Flux of Sensible Heat (Convection)		
H_C	$-p_2Bf_u(T_W - T_A)$	Wm^{-2}	
f_u	$4.4 + 1.82\sqrt{U_{10}^2 + V_{10}^2} + 0.26(T_W - T_A)$	$Wm^{-2}\ K^{-1}$	transfer function
U_{10}, V_{10}		$m\ s^{-1}$	wind speed at 10 m a.w.l.
B	0.61	-	Bowen coefficient
p_2	≈ 1.0	-	fit parameter
	Flux of Latent Heat (Evaporation, Condensation)		
H_E	$-f_u p_2\ (e_w - e_a)$		
e_w	$f_w \times 10^{\frac{0.7859+0.03477T_W}{1+0.00412T_W}}$	mbar	water vapor saturation pressure at temperature of water T_W
f_w	$0.61(1 + 10^{-6}p_a\ (4.5 + 6 \times 10^{-5}T_W^2))$	$W\ m^{-2}\ mbar^{-1}$	transfer function
p_a		mbar	air pressure

present parameterization of the heat fluxes is the result of a careful evaluation procedure of various parameterizations described in the literature [e.g., *Livingstone and Imboden*, 1989].

[23] As an alternative, the so-called sea surface temperature (*SST*) can be used as the boundary condition (Dirichlet type) for temperature at the water-atmosphere interface. Prescribing the *SST* as upper boundary condition has the advantage that the uncertainties in the estimation of H_{net} can be avoided. On the other hand, accurate and especially frequent *SST* measurements are not always available. In the ideal case *SST* is determined by one or more moored thermistors at the water surface with high accuracy and high repetition rate. Alternatively, *SST* can be obtained from regular in situ measurements (in general in weekly or monthly intervals) or from satellite observations.

[24] At the bottom boundary the boundary condition for temperature is given by the geothermal heat flux

$$\rho_0 c_p \left(\left(\nu_t' + \nu'\right) \frac{\partial T}{\partial z} \right)_{z_{bottom}} = H_{geo}. \tag{27}$$

Since the model is one dimensional, the flux of heat from the bottom area cannot be considered as boundary conditions, but is introduced in equation (1) as the production term.

[25] The absorption of shortwave radiation H_{sol} was calculated using the Lambert-Beer Law:

$$H_{sol} = H_{S_{sol,0}}(1 - r_s)e^{(-\epsilon_{abs}z)} \tag{28}$$

where $H_{Ssol,0}$ is the measured solar radiation above the water surface, r_s [-] and ϵ_{abs} [m^{-1}] are the reflection and extinction coefficient of the lake water. The latter can be approximated by

$$\epsilon_{abs} = \epsilon_{water} + \beta POC \tag{29}$$

where ϵ_{water} is the extinction coefficient of pure water ($\approx$0.3 m^{-1}), *POC* particulate organic carbon [mgPOC m^{-3}], and β the extinction coefficient of biomass ($\approx$0.00033 m^2 $mgPOC^{-1}$) [*Karagounis*, 1992].

2.3.2. Horizontal Velocity

[26] The upper boundary condition for horizontal velocity in x and y direction is given by the wind shear stress at the lake surface:

$$\rho_0 \left((\nu_t + \nu) \frac{\partial u}{\partial z} \right) = \tau_{surf,u} \qquad \rho_0 \left((\nu_t + \nu) \frac{\partial v}{\partial z} \right) = \tau_{surf,v} \tag{30}$$

The shear stress at the lake surface $\tau_{surf,u}$ $\tau_{surf,v}$ is given by

$$\left(\tau_{surf,u}, \tau_{surf,v}\right) = c_{10}\rho_{air}\left(v_{10}^2 + u_{10}^2\right)^{1/2}(v_{10}, u_{10}) \tag{31}$$

Unfortunately, literature values of c_{10} vary over a wide range and c_{10} depends on the state of surface waves and on wind speed. Moreover, for low wind speeds, measurements of the drag coefficient are relatively scarce [*Geerneart et al.*, 1988; *Bradley et al.*, 1991; *Simon*, 1997]. In this work, we took a value of $c_{10} = 1.3 \times 10^{-3}$, which is commonly used. At the bottom boundary horizontal velocities are assumed to be zero.

2.3.3. TKE and Dissipation

[27] As upper and bottom boundary conditions for k, the no-flux condition [*Burchard et al.*, 1998]

$$\left(\nu_k \frac{\partial k}{\partial z} \right)_{z_{surf}, z_{bottom}} = 0 \tag{32}$$

is used.

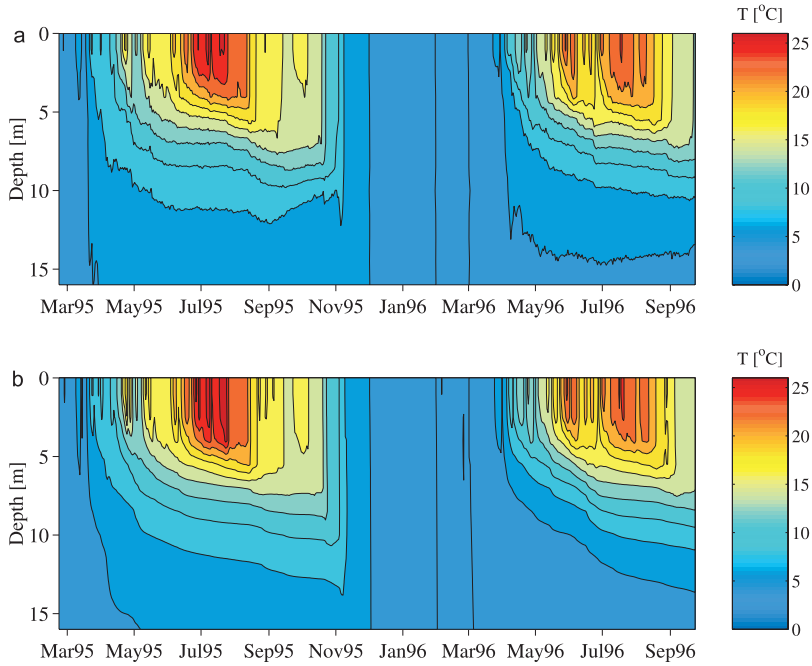

Figure 2. (a) Measured and (b) simulated temperature in Lake Baldegg in 1995–1996 using heat fluxes as boundary condition for temperature.

[28] As boundary conditions for ϵ we used the flux boundary condition of *Burchard and Petersen* [1999]

$$\left(\frac{\nu_t}{\sigma_\epsilon}\frac{\partial \epsilon}{\partial z}\right)_{z_{surf},z_{bottom}} = \left(c_\mu^0\right)^3 \frac{\nu_t}{\sigma_\epsilon}\frac{k^{3/2}}{\kappa(z+z_0)^2} \tag{33}$$

because it is numerically stable, yields reliable results even for course grids, and is physically well motivated. Here z is the distance from bottom or surface, z_0 the bottom or surface roughness length, and $\kappa = 0.41$ the von Kàrmàn constant.

2.4. Numerical Aspects

[29] The differential equations (1), (2), (3), and (4) have been integrated using the numerical scheme used by *Burchard and Baumert* [1995]. For the spatial discretization a staggered grid has been applied in which the water column is divided into a fixed number of not necessarily equidistant intervals. The mean flow quantities such as u, v, and T represent interval means and are placed in the center of the intervals. Turbulent quantities k and ϵ are defined at the interfaces between the intervals where they guarantee (in the case of equidistant intervals) a second order discretization of turbulent fluxes. Due to the absence of advection (and corresponding numerical diffusion) and the fully implicit treatment of diffusion, the time discretization is uncritical and an equidistant time stepping was used. A fully implicit integration algorithm (double sweep algorithm), which guarantees high numerical stability and high computational effectivity was implemented in the program. This makes the model also well suited for combined physical and biogeochemical studies on long timescales of several decades.

3. Application of the Model

3.1. Lake Baldegg

[30] In a first application, the thermal stratification and mixing processes in the upper layers of Lake Baldegg were modeled. Lake Baldegg is an eutrophic lake on the Swiss Plateau. It is approximately elliptical in shape and has a maximum depth of 65 m. Due to intense eutrophication problems (average P concentrations were up to 460 mg m^{-3} in 1974 [*Wehrli and Wüest*, 1996], the lake has been artificially oxygenated and aerated since 1982.

[31] The lake water temperature was measured quasi-continuously by a moored thermistor chain (Aanderaa, Bergen, Norway) at a sampling rate of 0.1 min^{-1} from 1 to 16 m depth during a nearly 2 year period from 1995 to 1996. Additionally, all model-relevant meteorological quantities (wind speed and direction, air temperature, humidity, and solar radiation) were measured at the same sampling rate by two weather stations (Aanderaa, Bergen, Norway) installed near the lake. At the lake surface the net heat flux H_{net} computed from measured meteorological quantities was used as boundary condition for the temperature equation. The parameters p_1, α, and q were determined by parameter optimization (Table 1).

[32] As shown in Figures 2, 3, and 4 the agreement between measured and simulated temperatures is very good. One of the reasons for the deviations during winter is the aeration which is not included in the model. The high-frequency temperature fluctuations in the thermocline and hypolimnion induced by internal seiches are not reproduced by the model, because this oscillating vertical motion is not explicitly included.

3.2. System Analysis

3.2.1. Model Evaluation

[33] As the evaluation of the model structure cannot be totally exhaustive, the comparison of model variants is restricted to two different boundary conditions for temperature, additional pressure gradients, and the extension of the standard k-ϵ by stability functions.

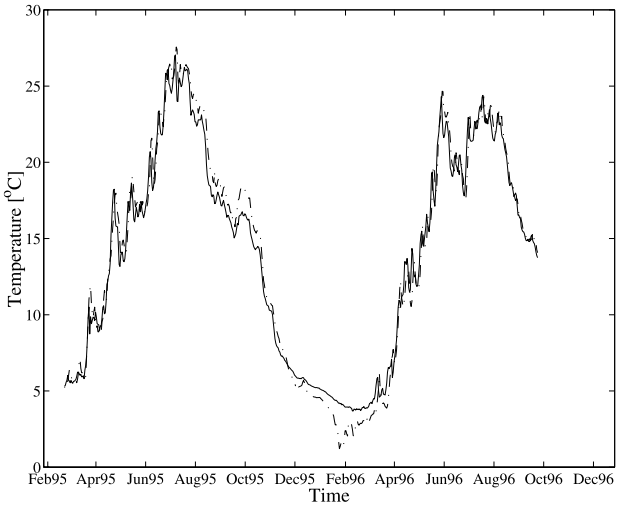

Figure 3. Measured (dotted line) and simulated (straight line) surface temperature in Lake Baldegg in 1995–1996 using heat fluxes as boundary condition for temperature.

[34] As mentioned above, as a good alternative to the prescription of heat flux at the water surface, also a Dirichlet type boundary condition for temperature can be used, i.e., surface temperature are directly given by measured values. Since in Lake Baldegg the uppermost thermistor was moored in 1 m depth, these measurements were used as an approximation for *SST* values, i.e., it was assumed that the surface layer in the upper one meter was completely mixed.

[35] As illustrated in Figures 2 and 4, results of the simulations using *SST* and heat fluxes as boundary condition for temperature agree both very well with the observations. For the simulations using *SST*, only the model parameters α and q had to be optimized. The corresponding parameter values differed only slightly from the previously obtained values (Table 1). The sum of the squared deviations using *SST* is considerably lower ($\approx$50%) compared to the value obtained using heat fluxes. However, this difference has its main origin in the upper layers where temporal variations in temperature dominate. These short-time fluctuations are (of course) exactly reproduced if *SST* is used as boundary condition. The main advantage of using *SST* as boundary condition is the fact that heat fluxes can only be computed indirectly from meteorological measurements using numerous bulk formulas and are difficult to determine accurately without optimizing the model parameter p_1 (and in some cases p_2) used in these formulas. However, if the response of the lake on climate variability is investigated or if no SST measurements are available, heat fluxes have to be used as boundary condition.

[36] For the standard k-ϵ model the stability functions c_μ and c'_μ are constants (Table 1). In order to include the limiting effect of stable stratification on diffusivity, c_μ and c'_μ depend on the (local) stability of the water column and are given by *Galperin et al.* [1988].

[37] In accordance with previous results in the literature [*Burchard et al.*, 1998], the extension of the standard k-ϵ model by incorporation of stability functions did not significantly affect the model results. Moreover, the numerical stability decreased when the stability functions were included. Most likely, these numerical difficulties are induced by the fact that stability functions tend to increase the stiffness of the partial differential equations. To avoid the additional numerical complications, we decided to restrict ourselves to the standard k-ϵ model for our applications. It should be noted that there are a few situations in which the buoyancy extension is able to improve considerably model results of dissipation rates above the bottom [*Burchard et al.*, 1998].

[38] As proposed by *Svensson* [1978], equation (2) can be extended by adding pressure gradients $-\frac{\partial p}{\partial x}$ and $-\frac{\partial p}{\partial y}$, respectively. Pressure gradients do not lend themselves to a simple treatment within a 1-D frame work. However, pressure gradients can be derived from simple 2-D models as shown by *Svensson* [1978]:

$$\frac{\partial p}{\partial x} = \int_{t_{start}}^{t_{sim}} \rho g \frac{\pi^2 \bar{u} h}{L_x^2} dt \qquad \frac{\partial p}{\partial y} = \int_{t_{start}}^{t_{sim}} \rho g \frac{\pi^2 \bar{v} h}{L_y^2} dt \tag{34}$$

where t_{start} and t_{sim} are start and actual simulation time, $\bar{u}$ and $\bar{v}$ vertically averaged velocities, h the average depth and L_x and L_y the average length in x and y direction of the basin.

[39] Including such pressure gradients result in nonvanishing horizontal velocities below the thermocline. However, only near the lake bottom at maximum depth, velocity gradients were increased significantly and induced shear stress and turbulent mixing. At other depths in the hypolimnion the contribution to turbulent mixing by the pressure-induced velocity gradients is negligible. Therefore, the

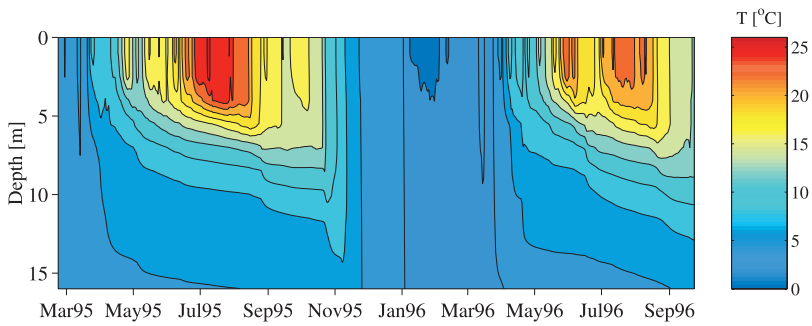

Figure 4. Simulated temperature in Lake Baldegg in 1995–1996 using *SST* as the boundary condition for temperature.

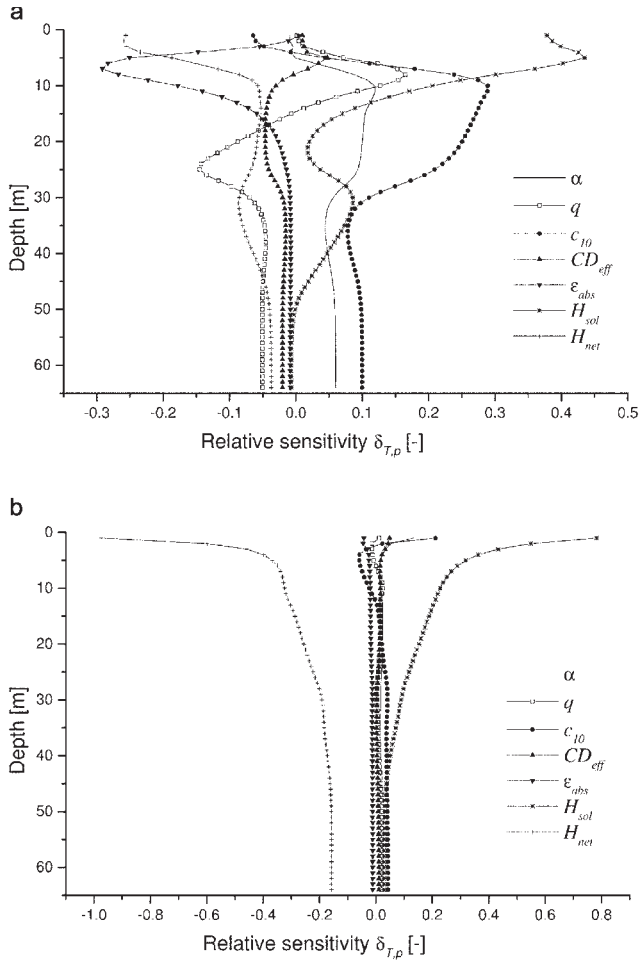

Figure 5. Relative sensitivity functions for temperature $\delta_{T,p}$ in Lake Baldegg averaged over (a) the stratified period (April 1 to December 1) and (b) the nonstratified period (December 2 to April 1).

additional pressure gradients were not included in the current version of the model.

3.2.2. Sensitivity Analysis

[40] In order to discuss the effect of the different parameters on the result of the simulation and to analyze the identifiability of the model parameters a sensitivity analysis was carried out. In linear approximation this was done by calculating the change of a variable y caused by a given change in a parameter p, i.e.,

$$\delta_{y,p} = \frac{p}{y}\frac{\partial y}{\partial p} \tag{35}$$

where $\delta_{y,p}$ gives the relative change in y for a 100% change in parameter $p = \alpha$, c_{10}, etc. The larger the value of the sensitivity function, the more accurately a single parameter p can be identified. A large sensitivity function also implies that the model results for y have a large uncertainty at a given uncertainty of the parameter p. The derivatives required for calculating the sensitivity functions are computed using the finite difference approximation

$$\frac{\partial y}{\partial p} \approx \frac{y(p+\Delta p) - y(p)}{\Delta p} \tag{36}$$

where Δp is chosen to be the standard deviation σ_p of the parameter p.

[41] In the case of several parameters, the sensitivity functions have to be linearly independent. Otherwise, the parameters are not individually identifiable, as a change in one parameter can be compensated for by changes in the other parameters. An alternative method, the nonlinear sensitivity analysis with the aid of Monte Carlo simulations, was not employed because of the large computational effort.

[42] The two model variables of most interest are temperature T and turbulent viscosity ν_t. As usually temperature is used to calibrate the model we only discussed the sensitivity functions for temperature.

[43] The sensitivity functions defined by equation (35) depend on time and depth. In order to discuss the overall role of the different parameters, the averaged sensitivity functions are shown in Figure 5 for the stratified (April 2 to December 1) and nonstratified situation (December 2 to April 1). For the sensitivity analysis only the parameters H_{net}, c_{10}, H_{sol}, ϵ_{abs}, α, q, and $C_{D_{eff}}$ were examined. The parameters of the k-ϵ model were not analyzed as these parameters have been already subject to several investigations in many other hydrodynamical situations [e.g., *Rodi*, 1984].

[44] As shown in Figures 5a and 5b the two parameters which dominate the temperature development at the surface are solar and longwave radiation H_{sol} and H_{net}. The sign of the sensitivity functions of the radiation is given by the sign of these terms itself, which is positive for H_{sol} and negative for H_{net}.

[45] During the nonstratified period, these terms dominate all others (Figure 5a), because mixing has hardly any effect on the temperature distribution and development if the whole water column is homogeneous. Consequently, the other parameters are difficult to determine during this period, as their impact on the result of the simulation vanishes compared to that of the radiation terms. During this period the two sensitivity functions of the radiation terms are linearly dependent, which indicates that these terms are difficult to determine independently of each other. The stronger increase of $\delta_{T,H_{net}}$ toward the surface compared to $\delta_{T,H_{sol}}$ is due to the fact that the solar radiation penetrates much deeper than infrared radiation, especially in winter when algae concentrations are small. Due to the lack of algae $\delta_{\epsilon_{abs}}$ is almost zero as mainly pure water absorbs radiation.

[46] During the stratified period (Figure 5b) the sensitivity functions vary much stronger, indicating that their identifiability is in general much better than during the nonstratified period. In the deep water near the bottom the temperature does not vary much with time and depth and the impact of the different parameters on temperature is generally small.

[47] As mixing in the epilimnion is mainly generated by direct wind forcing and convection, all parameters related to the seiche model (α and q) are almost zero in the upper 5 m and increase significantly in the thermocline.

[48] The sensitivity function of $C_{D_{eff}}$ is rather small for the entire water column and is approximately linearly dependent on the sensitivity function of α. One effect of $C_{D_{eff}}$ is that it determines how fast the potential seiche energy is damped (equation (14)). This affects the results of the simulations only on a short timescale and is averaged out during the whole stratified period. $C_{D_{eff}}$ also determines how

much of the kinetic energy of the seiche motion is dissipated within the viscous sublayer (equation (2)). Increasing $C_{D_{eff}}$ can therefore be compensated by increasing α and consequently, the value for $C_{D_{eff}}$ was not determined by parameter estimation but taken from the literature.

[49] The sensitivity functions $\delta_{T,c_{10}}$ and $\delta_{T,\alpha}$ are highly correlated below the surface layer depth as the production of seiche energy by wind forcing PW depends on both parameters (equation (10)). Only in the surface layer (approximately upper 5 m) $\delta_{T,\alpha}$ vanishes as mentioned above, whereas c_{10} remains important. Thus, it is basically possible to determine both parameters independently from each other, if a careful analysis of the upper surface layer is carried out. However, to reduce the number of estimated parameters, the value for c_{10} was taken from the literature and α was determined by parameter estimation.

[50] As the absorption of solar radiation in an eutrophic lake is mainly determined by the POC concentration, the sensitivity function $\delta_{T,\epsilon_{abs}}$ has its maximum in the upper thermocline where high POC concentrations induced by algae growth can be observed.

[51] The behaviour of $\delta_{T,q}$ is quite complex. In the surface mixed layer it vanishes for the same reason as $\delta_{T,\alpha}$. It increases in the upper thermocline as there the stability of the water column reaches its maximum and thus the input of kinetic seiche energy is focused there. Because of the stable stratification, increasing diffusivities will have a positive effect on temperature. At larger depths where the stability of the water column is lower, less kinetic seiche energy is transferred leading to a decrease in temperature. The 'z like' shape of the sensitivity function for q is nearly independent of all other parameters and q can be expected to be easily determined by parameter estimation in almost all stratified cases.

[52] $\delta_{T,H_{sol}}$ and $\delta_{T,H_{net}}$ show a similar behavior as during the nonstratified period. At the surface the structure of $\delta_{T,H_{sol}}$ is different because of the light absorption by POC. At a depth of approximately 30 m the profile of the sensitivity functions shows an unusual structure due to the complex distribution of kinetic seiche energy, as mentioned above.

[53] Summing up, the sensitivity analysis allows a systematic physical interpretation of all the model parameters and shows clearly which set of parameters can be determined by parameter estimation and for which parameters values have to be taken from literature.

3.2.3. Uncertainty Analysis

[54] One of the crucial aspects of modeling of environmental and technical systems is the ability to estimate the uncertainty of the model predictions. The thickness of the surface layer, which is mainly determined by the temperature stratification, is of central interest to biological and geochemical applications. To estimate the uncertainty of the model predictions for the thickness of the mixed surface layer, we used a simple error propagation method, where linearized propagation of standard deviation of uncorrelated parameters determines the uncertainty of the model results. The error propagation formula using the linearized model and neglecting parameter correlations is given by

$$\sigma_f = \sqrt{\sum_{i=1}^{m} \left(\frac{\partial T}{\partial p_i}\right)^2 \sigma_{pi}^2} \tag{37}$$

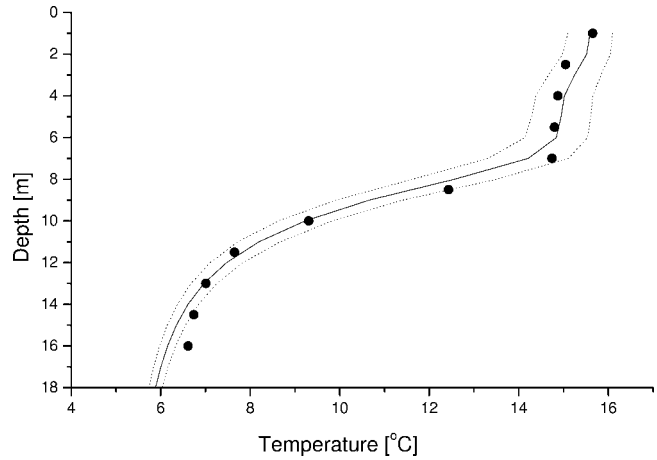

Figure 6. Simulated (solid line) and measured (dots) temperature in the upper 16 m of Lake Baldegg on October 5, 1995, with estimated error bounds (dotted lines).

where p_i are the uncertain model parameters, σ_{pi} their standard deviations, and σ_f the standard deviation of the model result. This method was used to determine the uncertainty of the model results for temperature T.

[55] Figure 6 shows the simulation results of the temperature distribution with estimated error bounds in the upper 16 m in Lake Baldegg on October 5, 1995, an arbitrary situation with a well-defined mixed layer. For the model parameters C_{10}, α, q, $C_{D_{eff}}$, ϵ_{abs}, and for the heat flux and solar radiation uncertainties of 10% were assumed. The measured temperature profile lies within the range of the predicted uncertainty for temperature, thus showing that the estimated uncertainty for T seems to be realistic. It should be noted that the prediction of the mixed layer depth has an uncertainty of approximately 1 m, which was also confirmed by uncertainty analysis for other lakes.

3.3. Lake Alpnach

[56] The application of the model to Lake Baldegg shows a good agreement between measurements and numerical results for the surface layer and the thermocline. In order to test the model also for the simulation of the temperature development in the hypolimnion, it was applied for Lake Alpnach during a period of approximately 3 weeks in summer (June 18 to July 9, 1995). Lake Alpnach, the smallest (surface area 4.8 km^2) basin of Lake Lucerne, is approximately elliptical in shape, relatively shallow (maximum depth of 34 m), and is separated from the main basin by a shallow sill. Lake Alpnach often experiences first and second vertical mode seiches [*Münnich et al.*, 1992]. As a consequence of the seiche currents, the benthic boundary layer is relatively well mixed and its thickness varies, depending on the depth and on the strength of the seiche oscillations, over a few meters [*Gloor et al.*, 1994]. Because of the low salinity gradients, the stratification of lake water is mainly controlled by temperature.

[57] During the entire time period, lake water temperature was measured quasi-continuously by two moored Aanderaa thermistor chains installed in series (from 1 to 11 m and 14 to 34 m depth) at the center of the lake. Additionally, all

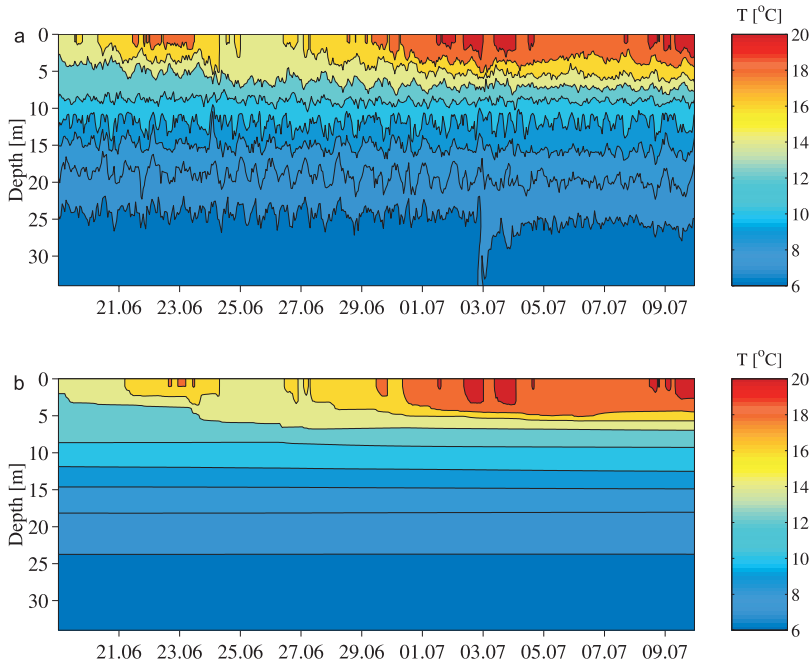

Figure 7. (a) Measured and (b) simulated temperature distribution for Lake Alpnach during the period from June 18 to July 10, 1995.

relevant meteorological quantities such as wind speed, air temperature, and solar radiation were measured by an Aanderaa weather station, installed at the airport near the lake. In Figure 7a, a contour plot of the measured temperatures illustrate the pronounced oscillations in the hypolimnion induced by seiching.

[58] As the focus in this case was the effect of internal seiching on vertical mixing, temperature measurements of the uppermost thermistor in 1 m depth were used as the boundary condition of temperature. As shown in Figure 7, the simulated temperatures agree very well with the observed values after adjusting parameter α and q (Table 1). In particular the agreement is excellent in both the epilimnion and thermocline. In the hypolimnion, the observed high-frequency oscillations were not reproduced, as these seiche-induced motions are not included explicitly in the model. However, on timescales larger than the typical seiche periods (several hours for the first vertical mode; 24 hours for the second vertical mode), deviations are relatively small.

[59] For most applications, the hypolimnetic development of temperature is not of primary interest. Instead, for geochemical or biochemical applications, the vertical structure and the temporal development of turbulent diffusivity in the hypolimnion is required. Therefore, based on temperature data, average turbulent diffusivities $\overline{\nu_t'}$ were calculated using the heat budget method of *Powell and Jassby* [1974].

[60] As shown in Figure 8, the modeled turbulent diffusivity averaged over the period of the measurements (June 18 to July 9, 1995) $\overline{\nu_t'}$ are in reasonable agreement with the values obtained using the heat budget method for the same period (dots). The measured turbulent diffusivities were reproduced similarly by the model not only in terms of absolute values but also the vertical structure agreed reasonably with the measurements.

[61] The deviations of the numerical results from the measurements may be attributed to the particular structure of the horizontal currents induced by the second vertical seiche mode, which is predominant in Lake Alpnach. Contrary to the common first vertical mode, this mode has a velocity structure with a maximum amplitude at approximately half of the basin depth. However, in the model it is assumed implicitly that the vertical structure of the seiche currents do not depend on depth. This is approximately the case for the first vertical seiche mode in the hypolimnion. Thus, the agreement in ν_t' can be expected to be even better in lakes where the first vertical mode is dominant.

4. Summary and Conclusions

[62] A one dimensional k-ϵ model has been adopted for the description of vertical fluxes in lakes. To describe the transport below the thermocline a model of the seiche energy balance and the production of TKE by the seiche motion was included. The results of this study revealed that the concept of bottom boundary mixing adequately describe vertical mixing processes below the thermocline. One of the most remarkable points of this study is the fact that the complex process of bottom boundary mixing can be parameterized by only two parameters in a one-dimensional model.

[63] Application to two different lakes, Lake Baldegg and Lake Alpnach, demonstrates that the model excellently describes the temperature distribution observed in these lakes on timescales between 3 weeks and 2 years. It was shown that additional pressure gradients and stability functions are not necessarily required to provide good agreement between model prediction and measurements. Minor disagreements were observed during periods when convection

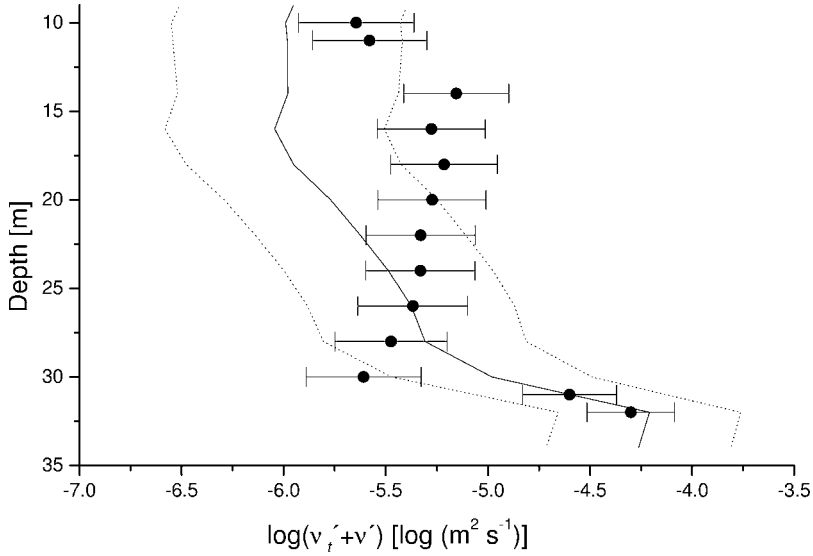

Figure 8. Comparison of average turbulent diffusivity calculated from temperature measurements using the heat budget method (dots) and simulated values (solid line). Standard errors are indicated by error bars (measurements) or dotted lines (simulations).

is dominant. Although model results for turbulent diffusivities are in reasonable agreement with values obtained using the heat budget method, it seems to be necessary to improve the parameterization of the vertical distribution of internal seiche energy with depth.

[64] By sensitivity analysis the physical interpretation of all model parameters was systematically shown. This analysis demonstrates which set of parameters have to be known from literature and which parameters can be determined by parameter estimation.

[65] Another results, worth to be emphasized, is the temporal dynamics of the kinetic energy of seiche motion. Model results of Lake Alpnach showed a decay time for E_{seiche} of approximately 3–4 days, in good agreement with experimental observations where a decay time of kinetic energy of the seiche motion of approximately 2–3 days was determined by current measurements [*Gloor et al.*, 2000].

[66] One of the important features of the implementation of the numerical model is its fast integration algorithm, which makes the model well suited for combined physical and biogeochemical studies on long timescales of several decades. Another advantage is the fact that the core of the model, the k-ϵ turbulence scheme, is derived from hydrodynamical equations which reduces the number of empirical relations. As vertical transport is computed from physical forcing, the lake model can also be applied to investigate the effect of climate change on stratification dynamics.

[67] On the basis of the promising results for Lake Baldegg and Lake Alpnach it can be concluded that the seiche-extended k-ϵ model may serve as a powerful tool for many combined physical-biogeochemical applications.

[68] In future studies, it is highly desirable to confirm the model structure by comparing modeled energy dissipation with experimental observations. Measurements of dissipation of TKE have become widely available through microstructure techniques. First preliminary studies indicate that measured diffusivities of TKE (e.g., by *Simon* [1997] in Lake Neuchatel) are in good agreement with TKE simulated with the model presented here. In addition, comparing long-term temperature observations with model predictions outside the calibration range will allow to evaluate the prognostic qualities of the model.

[69] **Acknowledgments.** This research was partially funded by Swiss National Science Foundation grants 2000-043357.95 and 20-50761.97 and by the Swiss Federal Office of Education and Science (BBW grant 97.0344) within the framework of the European Union Environment and Climate project REFLECT ('Response of European Freshwater Lakes to Environmental and Climatic Change') and CARTUM ('Comparative Analysis and Realization of second-order Turbulence Models', BBW grant 98.0169-1). We are indebted to Michael Schurter for his engagement in the field campaigns in Lake Baldegg and Lake Alpnach. We are grateful to P. Reichert for his ideas and suggestions and critical review of the manuscript.

References

Antenucci, J., J. Imberger, and A. Saggio, Seasonal evolution of the basin-scale internal wave field in a large stratified lake, *Limnol. Oceanogr.*, *45*, 1621–1638, 2000.

Barenblatt, G., Dynamics of turbulent spots and intrusions in a stably stratified fluid, *Izv. Atmos. Oceanogr. Phys.*, *14*, 139–145, 1978.

Bradley, E., P. Coppin, and J. Godfrey, Measurements of sensible and latent heat flux in the western equatorial Pacific Ocean, *J. Geophys. Res.*, *96*, 3375–3389, 1991.

Burchard, H., and H. Baumert, On the performance of a mixed-layer model based on the k-ϵ turbulence model, *J. Geophys. Res.*, *100*, 8523–8540, 1995.

Burchard, H., and O. Petersen, Models of turbulence in the marine environment—A comparative study of two-equation turbulence models, *Mar. Syst.*, *21*, 29–53, 1999.

Burchard, H., O. Petersen, and T. Rippeth, Comparing the performance of the Mellor-Yamada and the k-ϵ two-equation turbulence models, *J. Geophys. Res.*, *103*, 10,543–10,554, 1998.

Burchard, H., K. Bolding, and M. Villarreal, GOTM, a general ocean turbulence model: Theory, implementation and test cases, *Rep. EUR 18745*, 103 pp., Eur. Comm., 1999.

Crawford, G., and R. Collier, Observations of a deep-mixing event in Crater Lake, *Oreg. Limnol. Oceanogr.*, *42*, 299–306, 1997.

Elliott, A., Measurements of the turbulence in an abyssal boundary layer, *J. Phys. Oceanogr.*, *14*, 1778–1786, 1984.

Elliot, J., A. Irish, C. Reynolds, and P. Tett, Sensitivity analysis of PROTECH, a new approach in phytoplankton modelling, *Hydrobiologia*, *414*, 45–51, 1999.

Elo, A.-R., T. Huttula, A. Peltonen, and J. Virta, The effects of climate change on the temperature conditions of lakes, *Boreal Environ. Res.*, *3*, 137–150, 1998.

Galperin, B., L. Kantha, S. Hassid, and A. Rosati, A quasi-equilibrium turbulent energy model for geophysical flows, *J. Atmos. Sci.*, *45*, 55–62, 1988.

Garrett, C., The role of secondary circulation in boundary mixing, *J. Geophys. Res.*, *95*, 3181–3188, 1990.

Geerneart, G., K. Davidson, S. Larsen, and T. Mikkelsen, Wind stress measurements during the tower ocean wave and radar dependence experiment, *J. Geophys. Res.*, *93*, 13,913–13,923, 1988.

Gloor, M., Methode der Temperaturmikrostruktur und deren Anwendung auf die Bodengrenzschicht in geschichteten Wasserkörpern, Ph.D. diss., 159 pp., Eidg. Techn. Hochsh., Zürich, 1995.

Gloor, M., A. Wüest, and M. Münnich, Benthic boundary mixing and resuspension induced by internal seiches, *Hydrobiologia*, *284*, 59–68, 1994.

Gloor, M., A. Wüest, and D. Imboden, Dynamics of mixed bottom boundary layers in a stratified, natural water basin, *J. Geophys. Res.*, *105*, 8629–8646, 2000.

Goudsmit, G.-H., F. Peeters, M. Gloor, and A. Wüest, Boundary versus internal mixing in stratified natural waters, *J. Geophys. Res.*, *102*, 27,903–27,914, 1997.

Huttula, T., A. Peltonen, Ä. Bilaletin, and M. Saura, The effects of climatic change on lake ice and water temperature, *Aqua Fennica*, *22*, 129–142, 1992.

Imberger, J., Flux paths in a stratified lake: A review, in *Physical Processes in Lakes and Oceans*, *Coastal Estuarine Stud.*, vol. 54, edited by J. Imberger, pp. 485–502, AGU, Washington, D. C., 1998.

Imberger, J., and J. Patterson, A dynamic reservoir simulation model—DYRESM, in *Transport Models for Inland and Coastal Waters*, edited by H. Fisher, pp. 310–361, Academic, San Diego, Calif., 1981.

Imboden, D., and A. Wüest, Mixing mechanisms in lakes, in *Physics and Chemistry of Lakes*, pp. 83–138, Springer-Verlag, New York, 1995.

Karagounis, I., Ein physikalisch-biologisches Seemodell: Anwendung auf das Nordbecken des Luganersees, *VAW-Mitteilungen 116*, 156 pp., Lab. of Hydraul, Hydrol, and Glaciol, Zurich, 1992.

Karagounis, I., J. Trösch, and F. Zamboni, A coupled physical-biochemical lake model for forecasting water quality, *Aquat. Sci.*, *55*, 87–102, 1993.

Kraus, E., and J. Turner, A one-dimensional model of the seasonal thermocline, II, The general theory and its consequences, *Tellus*, *19*, 98–105, 1967.

Lemckert, C., and J. Imberger, Turbulent benthic boundary layer mixing events in fresh water lakes, in *Physical Processes in Lakes and Oceans*, *Coastal Estuarine Stud.*, vol. 54, edited by J. Imberger, pp. 503–516, AGU, Washington, D. C., 1998.

Livingstone, D., and D. Imboden, Annual heat balance and equilibrium temperature of Lake Aegeri, Switzerland, *Aquat. Sci.*, *51*, 1989.

MacIntyre, S., K. Flynn, R. Jellison, and J. Romero, Boundary mixing and nutrient flux in Mono Lake, *California. Limnol. Oceanogr.*, *44*, 236–242, 1999.

Münnich, M., A. Wüest, and D. Imboden, Observations of the second vertical mode of the internal seiche in an alpine lake, *Limnol. Oceanogr.*, *37*, 1705–1719, 1992.

Powell, T., and A. Jassby, The estimation of vertical eddy diffusivities below the thermocline in lakes, *Water Resour. Res.*, *10*, 191–198, 1974.

Ravens, T., O. Kocsis, A. Wüest, and N. Granin, Small-scale turbulence and vertical mixing in Lake Baikal, *Limnol. Oceanogr.*, *45*, 159–173, 2000.

Reynolds, C., and A. Irish, Modelling phytoplankton dynamics in lakes and reservoirs: The problem of in-situ growth rates, *Hydrobiologia*, *349*, 5–17, 1997.

Riley, M., and H. Stefan, Dynamic lake water quality simulation model 'Minlake,' *Tech. Rep. 263*, St. Anthony Falls Hydraul. Lab., Univ. of Minn.-Twin Cities, Minneapolis, 1987.

Rodi, W., Turbulence models and their application in hydrodynamics—A state of the art review, Univ. of Karlsruhe, Karlsruhe, Germany, 1984.

Simon, A., Turbulent mixing in the surface boundary layer of lakes, Ph.D. thesis, 99 pp., Eidg. Techn. Hochsh., Zürich, 1997.

Svensson, U., A mathematical model of the seasonal thermocline, Ph.D. thesis, Dep. of Water Resour. Eng., Lund Inst. of Technol., Univ. of Lund, Lund, Sweden, 1978.

Svensson, U., PROBE, program for boundary layers in the environment: System description and manual, *Tech. Rep. 24*, Swedish Meteorol. and Hydrol. Inst., Norrkping, 1998.

Ulrich, M., Modeling of chemicals in lakes—Development and application of user-friendly simulation software (MASAS and CHEMSEE) on personal computers, Ph.D. thesis, Eidg. Techn. Hochsh., Zürich, 1991.

Wehrli, B., and A. Wüest, Zehn Jahre Seenbelüftung: Erfahrungen und Optionen, *EAWAG Schriftenreihe 9*, Res., Teaching, Consult. for the Environ., Dübendorf, Germany, 1996.

Wüest, A., and M. Gloor, Bottom boundary mixing: The role of near-sediment density stratification, in *Physical Processes in Lakes and Oceans*, *Coastal Estuarine Stud.*, vol. 54, edited by J. Imberger, pp. 464–480, AGU, Washington, D. C., 1998.

Wüest, A., D. van Senden, J. Imberger, G. Piepke, and M. Gloor, Diapycnal diffusivity measured by microstructure and tracer techniques: A comparison, *Dyn. Atmos. Oceans*, *24*, 27–39, 1996.

Wüest, A., G. Piepke, and D. Van Senden, Turbulent kinetic energy balance as a tool for estimating vertical diffusivity in wind-forced stratified waters, *Limnol. Oceanogr.*, *45*, 1388–1400, 2000.

Zamboni, F., A. Barbieri, B. Polli, G. Salvade, and M. Simona, The dynamic model SEEMOD applied to the southern basin of Lake Lugano, *Aquatic Sci.*, *54*, 367–380, 1992.

G.-H. Goudsmit, F. Peeters, and A. Wüest, Swiss Federal Institute for Environmental Science and Technology (EAWAG), CH-8600 Dübendorf, Switzerland. (gerrit.goudsmit@axpo.ch)

H. Burchard, Institute for Oceanography, University of Hamburg, D-22529 Hamburg, Germany.